Bulletin of Earth Sciences of Thailand

Classification of Granitic Rocks Using Stained Rock and μ-XRF Analysis: Comparison with Lithogeochemical Data

Nannapat Kummoo[1], Ladda Tangwattananukul[1*] and Mayuko Fukuyama[2]

[1]Department of Earth Sciences, Faculty of Science, Kasetsart University, Bangkok 10900, Thailand
[2]Graduate School of Engineering Science, Akita University, Akita 010-8502, Japan

[*]Corresponding author e-mail: fscildt@ku.ac.th

Received: 07 Feb 2025
Revised: 11 Apr 2025
Accepted: 13 Apr 2025

ABSTRACT

The classification of granitic rocks has been approached using various methods by several researchers, considering limitations of grain size, texture and alteration. This research aims to present an effective technique for classifying fine-grained and slightly altered rocks. Modal analysis of three stained rock samples classifies them as alkali feldspar granite, while mineral composition analysis using μ-XRF also classifies them as alkali feldspar granite, with both methods yielding closely comparable mineral percentages. However, classification based on geochemical data differentiates the samples as monzogranite and syenogranite, revealing significant variations in alkali feldspar and plagioclase content. This discrepancy is likely influenced by alteration and weathering. Additionally, the geochemical method identifies minerals not observable in the samples, such as diopside and hematite, which further contribute to discrepancies in the CIPW norm. The μ-XRF element mapping of Al, Ca, Na, K, and Si provides insights into the morphology of quartz, plagioclase, and alkali feldspar, enhancing the understanding of mineral composition and paragenesis. This study proposes μ-XRF as a valuable method for improving the accuracy of rock classification under these constraints. While petrography and modal analysis remain fundamental, μ-XRF serves as a complementary technique, particularly for samples with similar limitations. The findings demonstrate that μ-XRF enhances the accuracy and reliability of granitic rock classification, especially for rocks with fine-grained samples.

Keywords: Pink granite, granitic rocks, staining technique, μ-XRF, CIPW norm

1. Introduction

Generally, intrusive and volcanic rocks can be classified by mineral composition, grain size, and texture, as seen in examples such as granite and rhyolite. The granitic rocks typically have medium to coarse grains and consist of quartz, feldspar, biotite, and mica. However, the occurrence of fine-grained granitic rocks remains a subject of ongoing investigation and discussion within the geological community (Migoń and Vieira., 2014; Zhang et al., 2022; Zhang et al., 2024). The crystallinity and morphology of minerals in granitic rocks play a significant role in identification rock types. Stained granitic rocks are commonly used for modal classification in the QAP diagram; however, the accuracy of rock type classification depends on factors such as the number of points counted for each mineral and the grain size. Modal analysis using the QAP diagram typically requires counting a minimum of 1,000 points. For greater precision, particularly in heterogeneous samples, some

studies recommend counting up to 2,000 points (Plas and Tobi, 1965). The accuracy of this method is influenced by visual limitations, which are affected by grain size, texture, and the degree of alteration on the rock surface. Alternatively, whole-rock geochemistry can be used to classify rock types through normative classification (CIPW norm) on the QAP diagram (Duchesne and Wilmart, 1997; Zeng et al., 2016; Shafaii et al., 2017; Nouri et al., 2018; Okunola et al., 2023). The CIPW norm is a method of converting the chemical composition of an igneous rock into an idealized mineral composition. This classification was devised by Cross et al. (1931) and allows for the discrimination of rock types in the slightly altered and weathered samples (Warren et al., 2007; Kapolas et al., 2024).

Various methods have been studied for classifying granitic rocks, including petrological analysis of thin sections, examination of mineral composition, modal analysis using rock staining techniques, and the whole-rock geochemistry (Lyons, 1971; Streckeisen, 1967, 1974; Frost et al., 2001). However, the classification of granitic rocks is influenced by grain size, which presents a limitation. For example, staining fine-grained rocks and dealing with textural variations make it difficult to visually identify minerals. Additionally, weathering and alteration affect the accuracy of major element concentrations in geochemical analyses.

Therefore, this study focuses on granitic rocks with varying grain sizes and the slightly alteration to identify the most suitable technique for classification granitic rocks. The aim is to investigate the minerals composition of granitic rocks by examining the grain size, shape and texture of minerals using petrography and modal analysis and comparing these findings with the elements distribution of mineral using μ-XRF analysis and the CIPW norm. This approach aims to propose an effective technique for classifying granitic rocks.

2. Geology

The study area is situated in Nong Bua District, Nakhon Sawan Province, central Thailand. The regional geology of the study area is predominantly composed of igneous and sedimentary rock (Figure 1). Permian sedimentary rocks, consisting of limestone, chert, shale, and sandstone are overlain by Permo-Triassic volcanic rocks, including rhyolite and andesite. These Permo-Triassic volcanic rocks are composed of volcanic and pyroclastic rocks including basalt, andesite, rhyolite, basaltic tuff, andesitic tuff, and lapilli tuff (Fanka and Nakapadungrat, 2018). Triassic granitic rocks are comprised of mica granite, tourmaline granite, granodiorite, mica granite, muscovite-tourmaline granite, and biotite-tourmaline granite (Figure 1b) (DMR, 2007). Various types of granitic rocks in Nong Bua area can be classified as monzodiorite, monzogranite, and alkali granite based on mineral composition (Fanka and Nakapadungrat, 2018).

Alkali granite is pink in color and characterized by fine-grained orthoclase, quartz, plagioclase, and biotite. Monzodiorite is white in color and consists of medium-grained quartz, plagioclase, K-feldspar, hornblende, and biotite. The rocks from study area are collected from Khao Phra-Khao Sung, Khao Lan Wua, and Khao Pak Rang corresponding to monzodiorite and alkali granite (Figure 1). These rocks vary in color, grain size and mineral texture.

3. Methodology

Samples were collected from Khao Phra-Khao Sung (sample no. A-1), Khao Lan Wua (sample no. A-2), and Khao Pak Rang (sample no. A-3) (Figure 1b). The samples were prepared as thin sections and stained slabs to determine their

mineral composition at the Department of Earth Sciences, Kasetsart University, Thailand. Minerals staining on rock surfaces for modal analysis was performed following the method described by Lyons (1971). In the modal analysis, major minerals such as quartz, alkali feldspar, and plagioclase were counted over 2000 points to determine their proportions, and the results were plotted on a QAP diagram. The rock samples were also analyzed using a micro-X-ray fluorescence (μ-XRF) instrument, the M4 Tornado (Bruker Nano), at Graduate School of Engineering Science, Akita University, Japan. The M4 Tornado operates at up to 50 kV and 800 μA; however, the polycapillary optics limit the detection of high-energy X-ray lines, such as the K-lines of barium (approximately 32–36 keV). An X-ray fluorescence spectrometer (XRF), Bruker Model AXS S4 PIONEER, located in the Department of Geology, Faculty of Science, Chulalongkorn University, was used to analyze the major and minor oxides of three samples. Rock standards JG-2, JB-3, AGV-2, GSP-2, BHVO-2, and RGM-1 were employed for calibration. Additionally, 1 g of powdered rock sample was used to determine the loss on ignition (LOI), measured before and after heating the samples at 950°C for 3 hours in a furnace. The whole-rock chemical composition of major and minor oxides was then used to calculate the CIPW norm (Tables 1 and 2) (Hollocher, 2004).

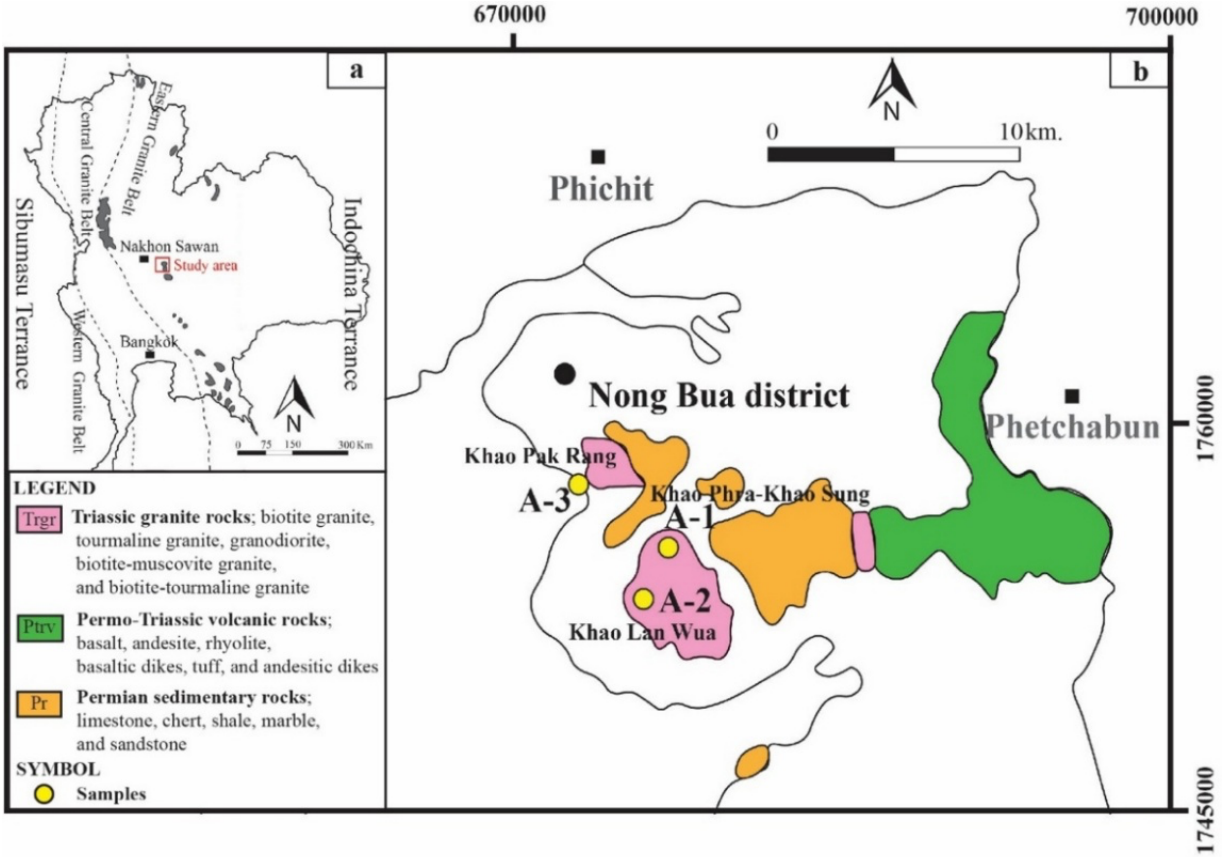

Figure 1 (a) Distribution of granitic rocks within the Eastern Granite Belt, extending from north to south of Thailand (Cobbing et al., 1986; Charusiri et al., 2002). The study area is in Nong Bua District, Nakhon Sawan Province, central Thailand. (b) Regional geology of Nong Bua District, Nakhon Sawan Province showing Permian sedimentary rocks and Permo-Triassic volcanic rocks intruded by Triassic granitic rocks (modified from DMR, 2007).

4. Results

4.1 Classification of granitic rocks by stained rocks

The modal analysis of three stained granitic rock samples classifies them as alkali feldspar granite, as shown in Figure 2.

Sample no. A-1 is a fine-grained granitic rock (0.5 to 2 mm), characterized by an equigranular texture which is composed of approximately 5.2% of plagioclase, 37.4% of quartz, 57.4% of alkali feldspar, and less than 1% of biotite and opaque mineral. Sample no. A-2 is a fine-grained granitic rock, consisting of approximately 5.6% of plagioclase, 38.7% of quartz, and 55.7% of alkali feldspar (Figure 2a-2d). The mineral composition comprises anhedral to subhedral quartz crystal (0.5 to 1 mm) and perthite grains (less than 1 mm), displaying a perthitic texture (Figure 3a-3d). Orthoclase displays lamellar twinning under cross-polarized light (Figure 3b). Plagioclase is a subhedral crystal with grain size less than 0.2 mm which is replaced by fine-grained quartz. Alkali feldspar mainly consists of perthite and orthoclase. It is anhedral, less than 1 mm in size, and shows a perthitic texture (Figure 3a-3d). Quartz is fine-grained and formed during the late stage of mineral crystallization. The fine-grained quartz is precipitated together with K-feldspar (Figure 3).

Alkali feldspar granite of sample no. A-3 is characterized by a medium-grained quartz, K-feldspar, plagioclase with trace amount of biotite and opaque minerals. The modal analysis of the stained rock reveals a composition of approximately 45.8% of quartz, 51.6% of alkali feldspar, and 2.6% of plagioclase (Figure 2f). Alkali feldspar, consisting of perthite and orthoclase is an anhedral to subhedral grains ranging from 2 to 4 mm in size and commonly exhibits a perthitic texture (Figure 3e and 3f).

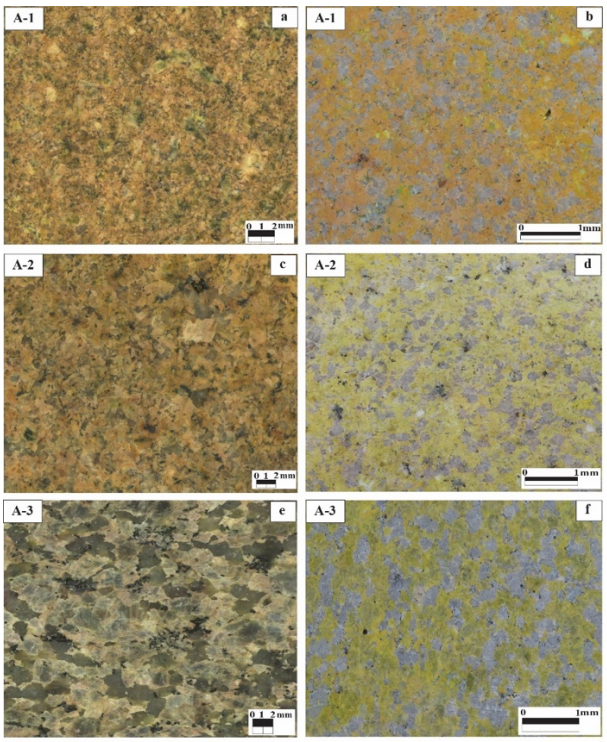

Figure 2 (a) Alkali feldspar granite of sample no A-1 is very fine-grain of mineral composition. (b) Stained of alkali feldspar granite of sample no. A-1. (c) alkali feldspar granite of sample no. A-2 is fine grain of quartz, feldspar and plagioclase. (d) Stained of alkali feldspar granite. (e) Alkali feldspar granite of sample no A-3 is medium grain of mineral composition. (f) Stained of alkali feldspar granite of sample no. A-3. Yellow refers to alkali feldspar, gray refers to quartz, and white refers to plagioclase.

Plagioclase is characterized by subhedral to euhedral crystals, ranging from 1 to 2 mm in size. Quartz can be separated into fine-grained and medium-grained varieties. The medium-grained quartz is subhedral to euhedral, with crystal sizes from 0.5 to 1 mm and occur as a late stage of mineral in the rock's composition. On the other hand, fine-grained quartz forms in the fractures among K-feldspar, plagioclase and

other quartz grains. Based on the grain size, texture and crystallinity of quartz, plagioclase, and alkali feldspar, it is difficult to accurately count the percentage of mineral composition from stained rocks for granitic rocks classification.

Table 1 Representative whole-rock geochemical analyses of granitic rocks in the Nong Bua area, Nakhon Swan (major and minor oxide in wt%).

Samples	A-1	A-2	A-3
Major oxide (wt%)			
SiO_2	76.73	76.09	73.41
TiO_2	0.07	0.08	0.22
Al_2O_3	11.93	12.04	11.90
Fe_2O_{3t}	1.01	1.19	3.19
MnO	0.00	0.02	0.06
MgO	0.07	0.07	0.25
CaO	0.33	0.38	0.93
Na_2O	3.97	4.07	4.56
K_2O	4.37	4.43	3.90
P_2O_5	0.01	0.01	0.03
LOI	0.77	0.76	0.74
Total	**99.27**	**99.13**	**99.20**

In the case of fine-grained granitic rocks, modal analysis using the staining technique was difficulty due to the visual limitations in distinguishing minerals, leading to errors. The modal composition of the medium-grained granitic sample was successfully determined, classifying it as alkali feldspar granite, with approximately of 46% of quartz, 52% of alkali feldspar, and 2% of plagioclase. To overcome the limitations associated with grain size in fine-grained samples, we employed digital image analysis by zooming in on high-resolution images and performing mineral point counting on a computer. This approach enabled the classification of the fine-grained granite as alkali feldspar granite, with an estimated composition of 38% of quartz, 56% of alkali feldspar, and 6% of plagioclase. However, this method is time-consuming.

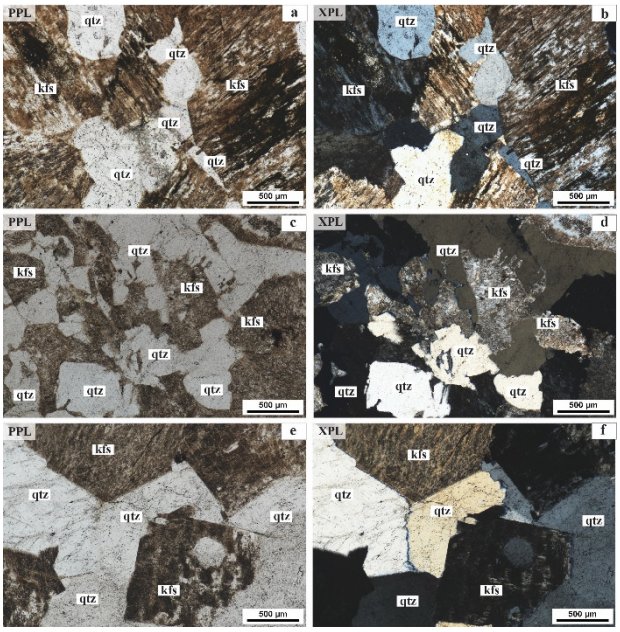

Figure 3 Photomicrographs of granitic rock under plane-polarized light (PPL) and cross-polarized light (XPL) for samples no. A-1, A-2, and A-3. (a-b) Alkali feldspar granite of sample no. A-1 showing perthitic texture of K-feldspar. Fine-grained anhedral quartz, K-feldspar. (c-d) Quartz is an anhedral to irregular in the K-feldspar crystal. (e-f) The alkali feldspar granite of sample no. A-3 exhibits a medium-grained perthitic texture in K-feldspar and anhedral shape of medium-grained quartz.

4.2 Classification of granitic rocks by µ-XRF analysis

The µ-XRF imaging reveals elemental variations in the granitic rocks which are related to mineral compositions in the rock samples. The distributions of Al, Ca, Na, K and Si are interpreted as quartz (SiO_2), plagioclase feldspar consists of albite ($NaAlSi_3O_8$) and anorthite ($CaAl_2Si_2O_8$), and alkali feldspar composed of K-feldspar ((K, Na) $AlSi_3O_8$), including microcline ($KAlSi_3O_8$), orthoclase ($KAlSi_3O_8$), anorthoclase ($(Na,K)AlSi_3O_8$) and perthite

($(K,Na)AlSi_3O_8$). These mineral compositions are used to classify types of granitic rocks using QAP diagram, identifying all three samples as alkali feldspar granite (sample no. A-1, A-2, and A-3) (Figures 4-6).

Qtz: quartz, kfs: K-feldspar), plg: plagioclase.

The distribution of Al, Ca, Na, K and Si can be combined to determine the major minerals compositions related to the paragenesis. Silicon is main element in quartz, K-feldspar and plagioclase. Aluminum, sodium, calcium and silicon combine to plagioclase. Silicon, aluminum, and potassium are interpreted as components of K-feldspar, while combination of silicon, aluminum, potassium, and sodium is indicative of alkali feldspar. These interpretations are useful for identifying alkali feldspar in the samples. Silicon is related to quartz which is shown in black color (Figures 4-5). The distribution of aluminum, sodium, and calcium corresponds with the presence of anorthite ($CaAl_2Si_2O_8$) and albite ($NaAlSi_3O_8$) (Figure 5a-5i). Interpretation of the images reveals mineral grains more clearly in medium-grained granitic rocks than fine-grained granitic rocks (Figure 5a and 5c). In addition, the distribution of each element can indicate the morphology of the minerals effected to crystallization sequence. The first mineral to crystallize in these granitic rocks is plagioclase, as indicated by the distribution of sodium. This is followed by alkali feldspar and K-feldspar, evidenced by the distribution of potassium and sodium, typically observed around the edges of plagioclase, and finally, quartz. Alkali feldspar granite of sample no. A-1 is composed of approximately 33.4% of quartz, 60.6% of alkali feldspar, and 6.0% of plagioclase. Alkali feldspar granite of sample no. A-2 consists of 39.3% of quartz, 54.7% of alkali feldspar, and 6.0% of plagioclase. Sample no. A-3 contains 44.0% of quartz, 52.7% of alkali feldspar and 3.3% of plagioclase (Figure 5). The μ-XRF imaging reveals elemental distributions in granitic rocks that correlate with their mineral compositions, specifically quartz, K-feldspar, alkali feldspar and plagioclase. These findings support the classification of the rocks as alkali feldspar granite based on the QAP diagram (Figure 6). The elemental distribution indicates the crystallization sequence, beginning with plagioclase, followed by alkali feldspar, K-feldspar, and finally quartz. Notably, fine-grained rocks exhibit less clear mineral grain boundaries compared to medium-grained rocks. A comparison between modal analysis of stained rock and the μ-XRF data for granitic rock classification confirms the same rock types. However, variations among all samples are observed in the closely percentages of major minerals (Figure 6). The combined μ-XRF elemental maps provide comprehensive information about the minerals present, allowing for the identification of perthite through the combination of silicon, aluminum, potassium, and sodium. This method enables a more accurate identification of alkali feldspar compared to the staining technique.

4.3 Classification of granitic rock by CIPW norm

The CIPW norm method first requires the conversion of mass-based oxide concentrations into mass mineral proportions using conventional normative calculations, followed by further conversion into volume proportions, which is necessary for QAP diagram classification (Stanley, 2017). The normative minerals identified in this method include sialic minerals (rich in silica and aluminum), such as quartz, corundum, orthoclase, and albite, as well as femic minerals (rich in iron and magnesium), such as hypersthene and diopside. Based on the

CIPW norm, the granitic rock samples were classified as follows: Sample A-1 was classified as monzogranite, with approximately 36.4% quartz, 27.6% orthoclase (K-feldspar), and 36% plagioclase. Sample A-2 was also classified as monzogranite, containing 37% quartz, 35.8% orthoclase (K-feldspar), and 27.2% plagioclase. Sample A-3 was classified as syenogranite, consisting of 25.6% quartz, 49.6% orthoclase (K-feldspar), and 24.8% plagioclase. Moreover, the CIPW norm results indentified only orthoclase, without accounting for other alkali feldspar minerals. Additionally, the method identified minerals not present in the samples, such as hematite and corundum, highlighting its limitations (Table 2). In comparison, the classifications obtained using the staining technique and the μ-XRF method are consistent with each other, showing the same classification types and similar mineral percentages. However, these results differ from the CIPW norm classification (Table 3).

5. Discussion

The classification of rocks obtained from the staining technique and the μ-XRF analysis, compared with the CIPW norm, suggests that the mineral composition percentages determined by point counting differ from those calculated from geochemical data (Figure 6). Limitations such as grain size, crystallinity, alteration, and mineral morphology have a small impact on the classification of granitic rocks when using the staining technique and μ-XRF analysis, as both techniques rely on visual identification. However, rock alteration and weathering significantly influence major and mobile trace elements, leading to discrepancies between the results obtained from the CIPW norm and those from staining and μ-XRF analyses. Additionally, the CIPW norm has inherent limitations, such as yielding only orthoclase without accounting for other alkali feldspar minerals and identifying minerals that are not present in the samples. These factors likely explain the differences observed between the results from the staining technique and μ-XRF analysis compared to the CIPW norm (Tables 2 and 3). Figure 6 presents the classification on the QAP diagram, comparing the modal analysis results obtained from the staining technique and the μ-XRF method. While slight differences in the percentage of major minerals were observed between the two methods, these variations are not systematic. The error between these two methods is approximately 5%.

Although the staining technique and μ-XRF analysis remain valuable approaches for classifying fine-grained granitic rocks, mineral identification and percentage estimation can be difficult (Stanley, 2017). Since granitic rock classification primarily depends on mineral proportions, various techniques can be used to determine these proportions, with both the staining technique and μ-XRF analysis being particularly effective for fine-grained rocks.

An alternative approach proposed by Le Maitre (1976) utilizes CIPW norms, calculated from geochemical data, to classify both plutonic and volcanic rocks on QAP diagrams. However, this method has certain limitations. CIPW norm calculations often yield mineral percentages for minerals that may not be present in the rock, such as corundum and hypersthene. Conversely, minerals commonly found in granitic rocks, such as biotite, muscovite, and hornblende, are not included as normative minerals (Stanley, 2017). Despite these limitations, the CIPW norm results from this study classified the samples as monzogranite and syenogranite.

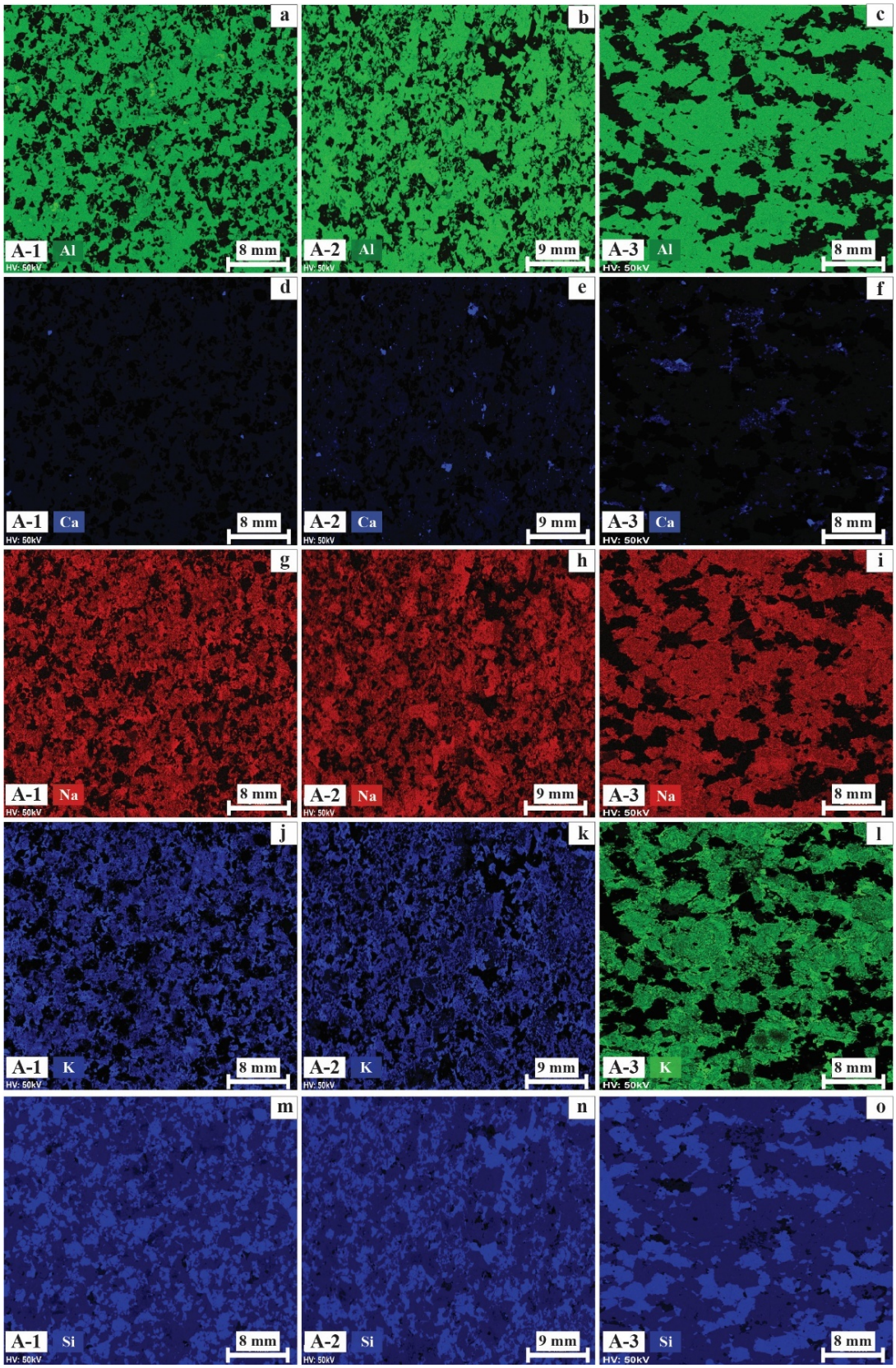

Figure 4 Elemental distribution images obtained through μ-XRF analysis, showing the spatial distribution of Al, Ca, Na, K and Si in samples no. A-1, A-2, and A-3.

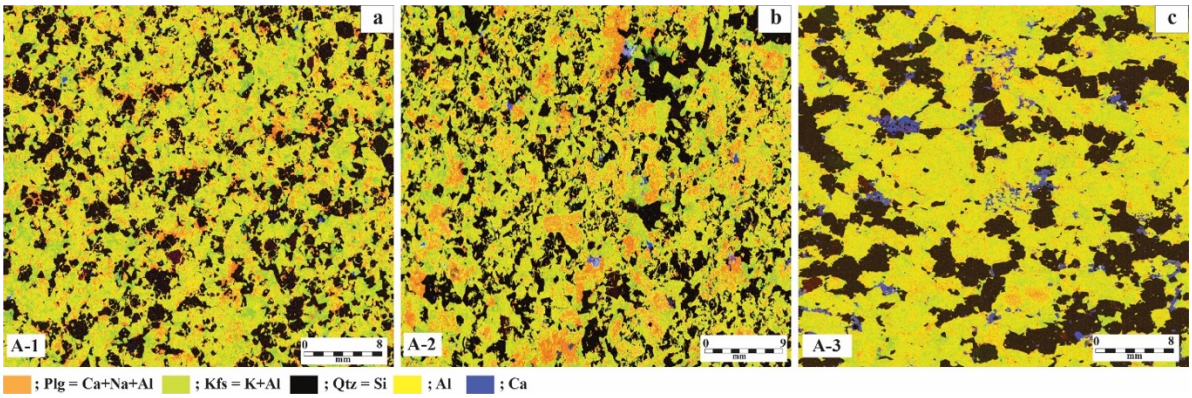

Figure 5 Combined elemental maps of Al, Ca, Na, K and Si obtained via the µ-XRF analysis, illustrating the distribution of quartz, alkali feldspar, plagioclase, Al and Ca in (a) sample no. A-1, (b) sample no. A-2, and (c) sample no. A-3.

Table 2 The results of the CIPW norm calculation from three granitic rocks samples in Nong Bua area, Nakhon Sawan province.

Samples	A-1	A-2	A-3	A-1	A-2	A-3
Normative mineral (Volume% Norm)				Recalculate to 100% (volume% norm)		
Quartz	34.89	36.25	23.21	36.40	37.00	25.60
Plagioclase	34.46	36.36	44.90	36.00	35.80	49.60
Orthoclase	26.59	25.77	22.34	27.60	27.20	24.80
Corundum	0.06	0.00	0.00			
Diopside	0.00	0.08	1.13			
Hypersthene	1.45	0.11	0.00			
Wollastonite	0.00	0.00	0.67			
Rutile	0.04	0.07	0.00			
ilmenite	0.00	0.02	0.07			
Hematite	0.51	0.61	1.65			
Apatite	0.02	0.02	0.06			
Zircon	0.00	0.00	0.00			
Sphene	0.00	0.11	0.29			

Table 3 The classification types of granitic rocks using staining technique, µ-XRF analysis and CIPW norm.

Sample no.	**Methods**	**Mineral compositions (%)**			**Type of rocks**
		Quartz	**Alkali feldspar**	**Plagioclase**	
A-1	Staining technique	37.4	57.4	5.2	Alkali feldspar granite
	µ-XRF analysis	33.4	60.6	6.0	
	CIPW norm	36.4	27.6	36.0	Monzogranite
A-2	Staining technique	38.7	55.7	5.6	Alkali feldspar granite
	µ-XRF analysis	39.3	54.7	6.0	
	CIPW norm	37.0	35.8	27.2	Monzogranite
A-3	Staining technique	45.8	51.6	2.6	Alkali feldspar granite
	µ-XRF analysis	44.0	52.7	3.3	
	CIPW norm	25.6	49.6	24.8	Syenogranite

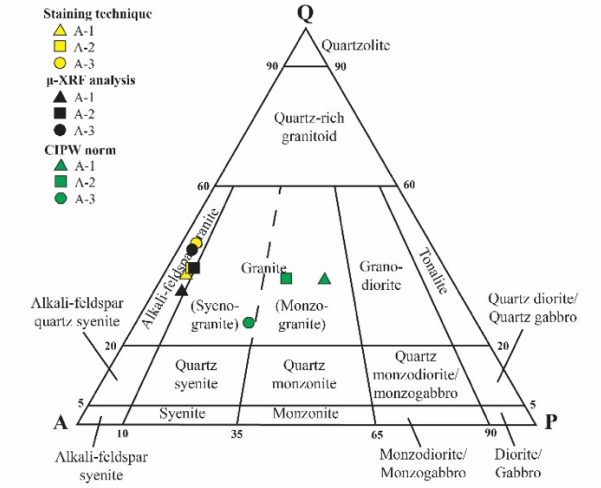

Figure 6 QAP classification diagram for granitic rocks in the Nong Bua area using staining techniques, the μ-XRF analysis, and the CIPW norm (Streckeisen, 1974). (Q: quartz, A: alkali feldspar, P : plagioclase).

These results suggest that different types of granitic rocks can be identified, with an error comparable to both methods approximately 15–20%. Most samples show similar percentages of quartz, while the proportions of plagioclase and alkali feldspar exhibit more variability (Table 3). This variability is influenced by the alteration and weathering of rock samples. Additionally, as shown in Table 2, the normative minerals provided by the CIPW norm are limited, as it identifies only orthoclase and fails to account for other alkali feldspars. The CIPW norm also detects minerals, such as corundum and hypersthene, that should not be present in granitic rock samples. These discrepancies highlight the differences in the proportions of plagioclase and alkali feldspar identified by the staining technique and μ-XRF analysis, compared to the results obtained from the CIPW norm. This error is influenced by factors such as the degree of rock alteration and the selection of the granitic rock powder. It is essential to choose a homogeneous, fresh, or at slightly altered, rock sample for powdering.

In addition, the study by Stanley (2017) suggested that geochemical classification can distinguish between metaluminous I-type granites and peraluminous S-type granites, serving as an alternative to traditional methods such as visual estimation, point counting, image analysis, and spectrometric mineral mode-based Streckeisen classification. However, the granitic rocks in the Nong Bua area fall within the transition of magmatic activity to form I-type to S-type granites composition (Kummoo and Tangwattananukul, 2022). Despite this, the geochemistry of the studied samples is insufficient for accurate classification on QAP diagram is not suitable for the samples which presents the alteration. It can be suggested the staining technique and the μ-XRF method should be used together for classifying granitic rocks, especially under limitations of grain size, texture and alteration. Although both methods are time-consuming, the μ-XRF method provides valuable information by revealing the distribution of elements such as Al, Ca, Na, K, and Si, which can help identify the end-members of the two feldspar solid solutions. Furthermore, the distribution maps generated by the μ-XRF can offer insights into the paragenesis of minerals, aiding in the understanding of crystallization sequences. This method also facilitates the identification of complex minerals with poor crystallinity. In the case of altered rocks, the μ-XRF method can detect elements still present in the sample, including trace elements, which can be used to study accessory minerals that are not easily visible to the naked eye.

6. Conclusion

The classification of three granitic rock samples from the study area, considering variations in grain size, texture, and slightly

alteration, was conducted using staining techniques, the μ-XRF analysis, and CIPW norm calculations. Both the modal analysis of stained rocks and μ-XRF data classified the granitic rocks as alkali feldspar granite. However, the CIPW norm yielded a different rock classification, likely due to the effects of alteration and weathering. Therefore, the use of staining techniques, the μ-XRF analysis was sufficient for classification of granitic rock with varying textures and grain sizes. Moreover, μ-XRF analysis can be used to access paragenesis of minerals and allows for the identification of each mineral of interest.

7. Acknowledgments

This research was partially funded by the Development and Promotion of Science and Technology Talented Project (DPST), Thailand, under grant 2024. We also thank Graduate School of Engineering Science, Akita University, Japan for suggestions in preparing and analyzing the μ-XRF data. The authors would like to thank the reviewers for their careful reading of our manuscript and their constructive comments. Finally, we sincerely thank the Department of Earth Science, Faculty of Science, Kasetsart University, for their continued support.

8. References

Charusiri, P., Daorerk, V., Archibald, D., Hisada, K.-I. and Ampaiwan, T. 2002. Geotectonic evolution of Thailand: A new synthesis. Journal of the Geological Society of Thailand, 1, 1-20.

Cobbing, E.J., Mallick, D.I.J., Pitfield, P.E.J. and Teoh, L.H. 1986. The granites of the Southeast Asian Tin Belt. Journal of the Geological Society, 143, 3, 537-550.

Department of Mineral Resources. 2007. Geologic map of Nakhon Sawan Province with 1: 250,000 ratios.

Duchesne, J.G. and Wilmart, E. 1997. Igneous Charnockites and Related Rocksfrom the Bjerkreim–Sokndal Layered Intrusion (Southwest Norway): a Jotunite (Hypersthene Monzodiorite)-Derived A-type Granitoid Suite. Journal of Petrology 38, 3, 337-369.

Fanka, A. and Nakapadungrat., S. 2018. Preliminary Study on Petrography and Geochemistry of Granitic Rocks in the Khao Phra -Khao Sung area, Amphoe Nong Bua, Changwat NakhonSawan, Central Thailand. Journal of Bulletin of Earth Science of Thailand 10, 55 – 68.

Frost, B., Barnes, C., Collins, W., Arculus, R., Ellis, D. and Frost, C. 2001. A Geochemical Classification for Granitic Rocks. Journal of Petrology 42, 2033-2048.

Kapolas, A., Finzel, E.S., Horkley, L.K. and Peate, D.W. 2024. The effects of weathering and sediment source mixing on whole-rock geochemical provenance studies, Cook Inlet forearc basin, south-central Alaska, USA. GSA Bulletin 136, 9-10, 4353-4363.

Kummoo, N. and Tangwattanukul L. 2022. Geochemistry of Granitoids at Nong Bua District, Nakhon Sawan Province, Thailand in press. 48th International Congress on Science, Technology and Technology-based Innovation (STT48), School of Science Walailak University, Nakhon Si Thammarat, Thailand.

Le Maitre, R.W. 1976. The chemical variability of some common igneous rocks. Journal of Petrology, 17, 589–637.

Lyons, PC. 1971. Staining of feldspars on rock-slab surfaces for modal analysis. Mineralogical Magazine 38, 518-519.

Migoń, P. and Vieira, G. 2014. Granite geomorphology and its geological controls, Serra da Estrela, Portugal. Journal of Geomorphology 224, 1-14.

Nouri, S.F., Azizi, H., Stern, B., Asahara, Y., Khodaparast, S., Madanipour, S., and Yamamoto, K. 2018. Zircon U-Pb dating, geochemistry and evolution of the Late Eocene Saveh magmatic complex, central Iran: Partial melts of sub-continental lithospheric mantle

and magmatic differentiation. Journal of Lithos 314-315, 274-292.

Okunola, O., Olatunji, A. and Adegoke, A. 2023. Geology and Rare Earth Element Geochemistry of Magnesian Granitoids Within Proterozoic Schist Belt of Southwest Nigeria. Journal of Materials and Geoenvironment 69,2, 1-19.

Plas, L. van der and Tobi, A.C. 1965. A chart Judging the Reliability of Point Counting Results. America Journal of Science 263, 87-90.

Shafaii, M.H., Griffin, W., Li, X., Santos, J.F., Karsli, O., Stern, B., Ghorbani, G., Gain, S., Murphy, R. and O'Reilly, S. 2017. Crustal Evolution of NW Iran: Cadomian Arcs, Archean Fragments and the Cenozoic Magmatic Flare-Up. Journal of Petrology 58, 11, 2143-2190.

Stanley, C. 2017. Lithogeochemical classification of igneous rocks using Streckeisen ternary diagrams. Geochemistry: Exploration, Environment, Analysis 17, 463.

Streckeisen, A. 1967. Classification and nomenclature of igneous rocks. Nues Jarbuch fur Mineralogie Abhandlungen 107, 144-240.

Streckeisen, A. 1974. Classification and nomenclature of plutonic rocks recommendations of the IUGS subcommission on the systematics of Igneous Rocks. Geologische Rundschau 63, 773 –786.

Streckeisen, A.L., Zanettin, B.A., LE Bas, M.J., Bonin, B., Bateman, P., Bellineni, G., Dudek, A., Efremova, S., Keller, J., Lameyre, J., Sabine, P.A., Schmid, R., Sorensen, H. and Woolley, A.R. 2002. Igneous Rocks; A Classification and Glossary of Terms; Recommendations of the International Union of Geological Science Subcommission on the Systematics of Igneous Rocks. Cambridge University Press, Cambridge.

Warren, I., Simmons, S.F. and Jeffrey L.M. 2007. Whole-Rock Geochemical Techniques for Evaluating Hydrothermal Alteration, Mass Changes, and Compositional Gradients Associated with Epithermal Au-Ag Mineralization. Economic Geology 102, 923-948.

Zeng, Q., Guo, W., Chu, S. and Duan, X. 2016. Late Jurassic granitoids in the Xilamulun Mo belt, Northeastern China: Geochronology, geochemistry, and tectonic implications. International Geology Review 58, 1-15.

Zhang, T., Xia, Q., Yang, X., Zhao, Z., Sun, J., Zha, X. and Lu, Y. 2024. The petrogenesis and metallogenesis of the ore-forming granites in the Tongmukeng Sn deposit, Jiangnan Orogenic Belt, South China. Journal of Ore Geology Reviews 168, 1-16.

Zhang, Z., Zhang, D., Xiang, X., Zhu, X. and He, X. 2022. Geology and mineralization of the supergiant Shimensi granitic-type W-Cu-Mo deposit (1.168 Mt) in northern Jiangxi, South China: A Review. Journal of China Geology 5, 3, 510-527.